

Compositional tuning of the strain-induced structural phase transition and of ferromagnetism in $\text{Bi}_{1-x}\text{Ba}_x\text{FeO}_{3-\delta}$

Charlee J.C. Bennett

Materials Science and Technology Division, Oak Ridge National Laboratory, Oak Ridge, Tennessee 37831

Hyun Sik Kim

Materials Science and Technology Division, Oak Ridge National Laboratory, Oak Ridge, Tennessee 37831; and Department of Physics, University of Warwick, Coventry CV4 7AL, United Kingdom

Maria Varela

Materials Science and Technology Division, Oak Ridge National Laboratory, Oak Ridge, Tennessee 37831

Michael D. Biegalski

Center for Nanophase Materials Sciences, Oak Ridge National Laboratory, Oak Ridge, Tennessee 37831

Dae Ho Kim

Materials Science and Technology Division, Oak Ridge National Laboratory, Oak Ridge, Tennessee 37831; and Department of Physics, Tulane University, New Orleans, Louisiana 70118

David P. Norton

Department of Materials Science and Engineering, University of Florida, Gainesville, Florida 32611

Harry M. Meyer III

Materials Science and Technology Division, Oak Ridge National Laboratory, Oak Ridge, Tennessee 37831

Hans M. Christen^{a)}

Materials Science and Technology Division, Oak Ridge National Laboratory, Oak Ridge, Tennessee 37831; and Center for Nanophase Materials Sciences, Oak Ridge National Laboratory, Oak Ridge, Tennessee 37831

(Received 9 November 2010; accepted 18 February 2011)

Recent studies by a number of research groups have shown that the structure of epitaxial BiFeO_3 (BFO) films changes drastically as a function of substrate-induced biaxial compression, with the crystal structure changing from one being nearly rhombohedral (R-like) to one being nearly tetragonal (T-like), where the “T-like” structure is characterized by a highly enhanced c/a ratio of out-of-plane c to in-plane a lattice parameters. In this work, we show that the critical compressive strain σ_c necessary to induce this transition can be reduced significantly by substituting 10% Ba for Bi [$\text{Bi}_{0.9}\text{Ba}_{0.1}\text{FeO}_{3-\delta}$ (BBFO)] and that the “T-like” phase in both BBFO and BFO is stable up to the decomposition temperatures of the films in air. Furthermore, our results show that the BBFO solid solution shows clear ferromagnetic properties in contrast to its undoped BFO counterpart.

I. INTRODUCTION

Bismuth ferrite [BiFeO_3 (BFO)]¹ is the only known material with both magnetic order and a large ferroelectric polarization at room temperature. This makes this perovskite compound singularly interesting both for applications (sensors or spintronics) and from the perspective of scientific interest in the coexistence of magnetic and polar properties that are often seen as mutually exclusive.² The recent experimental observation of a highly tetragonal phase in BFO films with $c/a > 1.2$ ^{3–6} is promising for the development of lead-free piezoelectric materials and illustrates the strong structural changes that can be induced via epitaxial strain.

The use of strain and composition is an attractive method for tuning properties of materials in thin-film form. The dependence of the ferroelectric polarization in BFO on strain has been studied both experimentally^{7,8} and theoretically^{6,8} and reveal that the polarization (pointing in a 111 direction in the bulk) rotates toward the 001 axis under mild compressive strain, $-0.5\% < \sigma$, yielding a significant increase in the polarization measured along the 001 direction. However, larger compressive strain ($-3\% < \sigma < -0.5\%$)^{6,7} results in only a weak further increase. Perhaps the most surprising feature is the observation of an apparently highly tetragonal phase under much larger compressive strain ($\sim -5\%$).^{3–6} In fact, while BFO grown on a variety of substrates is monoclinic^{9–11} but close to rhombohedral, with a pseudo-cubic c/a ratio close to unity (R-like phase), the material transforms to monoclinic but close to tetragonal, with $c/a > 1.2$ (T-like phase), when grown under large compressive strain.^{4–6}

^{a)}Address all correspondence to this author.

e-mail: christenhm@ornl.gov

DOI: 10.1557/jmr.2011.59

In other words, strain induces monoclinic-to-monoclinic phase transition in BFO (which is, however, not strictly isosymmetric¹²).

This remarkable strain-driven structural phase transition occurs only when BFO is grown on substrates with an in-plane lattice parameter below ~ 3.8 Å (see below). However, such large compressive strain is difficult to achieve on many of the commercially available substrates and conducting oxide bottom electrodes, and even growth onto LaAlO_3 substrates may not always yield single-phase films.⁵ In fact, clear demonstration of ferroelectric switching via polarization-field ($P(E)$) hysteresis loops has so far only been achieved on Mn-doped films.⁴ This motivates us to explore ways to tune the critical strain σ_c necessary to induce the transition via a modification of the unit cell volume by substitution of a larger ionic radius cation for either Bi or Fe. Ba substitution is particularly intriguing as the alloys between the antiferromagnetic/ferroelectric BFO and BaFeO_{3-y} ¹³⁻¹⁷ are expected to exhibit interesting physical properties on their own right: $\text{BaFeO}_{2.5}$ (Fe³⁺) is a paramagnetic insulator (C.J.C. Bennett, unpublished data), whereas the perovskite form of BaFeO_3 (Fe⁴⁺) is theoretically predicted to be a ferromagnetic insulator,^{13,18-21} with a ferromagnetic Fe⁴⁺-O-Fe⁴⁺ super-exchange coupling. Epitaxial films of BaFeO_{3-x} ($x < 0.5$) indeed show ferromagnetic behavior²² even though oxygen vacancies will result in a mixed Fe valence state and are the subject of further study (C.J.C. Bennett, unpublished data).

In this work, we show that the critical compressive strain σ_c necessary to induce the transition from the R-like to the T-like phase can be reduced significantly in a 10% Ba-substituted alloy ($\text{Bi}_{0.9}\text{Ba}_{0.1}\text{FeO}_{3-\delta}$). This solid solution shows clear ferromagnetic properties. We also demonstrate that the T-like phase in both BBFO and BFO is stable up to the decomposition temperatures of the films in air.

II. EXPERIMENTAL METHODS

Epitaxial films of $\text{Bi}_{1-x}\text{Ba}_x\text{FeO}_{3-\delta}$ were grown by pulsed laser deposition onto a variety of substrates [SrLaAlO_4 ($a = 3.755$ Å), LaAlO_3 (LAO) (pseudocubic lattice parameter $a_{pc} = 3.789$ Å), NdGaO_3 (NGO) ($a_{pc} = 3.85$ Å), $(\text{La}_{0.29}\text{Sr}_{0.71})(\text{Al}_{0.65}\text{Ta}_{0.35})\text{O}_3$ (LSAT) ($a = 3.86$ Å), SrTiO_3 ($a = 3.905$ Å), and KTaO_3 (KTO) ($a = 3.989$ Å)]. All substrates were cut in a pseudocubic 001 orientation. To explore the entire composition range ($0 \leq x \leq 1$), repeated alternating deposition of sub-monolayer amounts of BFO and BaFeO_{3-y} were used (two-target mixing²³), while an additional series of samples with $x = 0.1$ was grown using a $\text{Bi}_{0.9}\text{Ba}_{0.1}\text{FeO}_{3-\delta}$ solid solution target. X-ray photoelectron spectroscopy (XPS) measurements (data not shown, see below) confirmed the correct Ba content in the samples obtained by

two-target mixing. All films were grown at 700 °C in a background gas of 50 mTorr O₂, a laser repetition rate of 10 Hz, and a deposition rate of ~ 0.17 Å per laser pulse. Typical film thicknesses were 80–100 nm. The films' structure was analyzed via high resolution x-ray diffraction (XRD, PANalytical X'Pert MRD, Almelo, The Netherlands) and at variable temperature. SQUID magnetometry (Quantum Design MPMS, San Diego, CA) was used to measure the magnetic properties. Electron microscopy observations were carried out in a VG Microscopes HB501UX equipped with a Nion aberration corrector and operated at 100 kV. Specimens were prepared by conventional grinding and ion milling. Composition and valence state information were obtained by XPS using a K-Alpha XPS instrument (Thermo Fisher Scientific, Waltham, MA) using a monochromatic Al K α x-ray source focused to a 400 μm diameter spot on the sample surface, with the data acquired at a pass energy of 50 eV on samples sputter etched for 15 s using 1 kV Ar ions.

III. RESULTS AND DISCUSSION

A. Structure of $\text{Bi}_{1-x}\text{Ba}_x\text{FeO}_{3-\delta}$ films

Figure 1(a) shows in-plane (a) and out-of-plane (c) lattice parameters for the entire composition range, $0 \leq x \leq 1$, as extracted from reciprocal space maps (RSMs) containing the substrate's and the film's pseudocubic 013 diffraction peak. Samples for $x \geq 0.2$ were grown onto relaxed films of SmScO_3 ($a_{pc} = 3.99$ Å) on LaAlO_3 substrates, whereas those for $x \leq 0.1$ were deposited onto KTaO_3 substrates. In other words, substrates or buffer layers with large in-plane lattice parameters were chosen in all cases to minimize compressive strain. Single-phase solid-solution films were obtained for all values of x . Figure 1(a) also shows the corresponding unit cell volume (plotted as $V^{1/3} = (a^2c)^{1/3}$). Although there is a significant amount of scatter on the data points, the general trend of the unit cell volume clearly follows the expectation from Vegard's law (solid line). The horizontal line indicates the lattice parameter of the SmScO_3 buffer layer, showing that the samples in a range near $x = 0.5$ are somewhat "clamped" to this buffer layer, whereas structural relaxation is apparent both at higher and lower values of x . All films crystallize in a perovskite crystal structure that can approximately be described as tetragonally distorted. On these SmScO_3 or KTaO_3 templates with $a = 3.99$ Å, we find that the tetragonality remains small, with $c/a < 1.03$ even at $x = 1$, where the distortion is largest.

The RSMs for all these films grown on SmScO_3 or KTaO_3 are characterized by a single peak for the 103_{pc} and 113_{pc} reflections (with some broadening occurring as a consequence of a small monoclinic distortion, as is typically seen for BFO⁹⁻¹²). A completely different picture arises when films with $x = 0.1$ are grown onto various substrates with different in-plane lattice parameters. As

shown in Fig. 1(b), for $\text{Bi}_{0.9}\text{Ba}_{0.1}\text{FeO}_{3-\delta}$ grown on LSAT, the 103_{pc} peak splits into two well-separated reflections corresponding to one in-plane lattice parameter ($a = 3.86 \text{ \AA}$) but two out-of-plane lattice parameters (4.24 \AA and 4.38 \AA , respectively). When grown on LaAlO_3 , i.e., a substrate with an even smaller lattice parameter, a single peak is found again, as shown in Fig. 1(c), with $a = 3.79 \text{ \AA}$ and $c = 4.64 \text{ \AA}$. Figure 1(d) shows a Z-contrast scanning transmission electron microscopy image of this film. It is clearly seen that this film grows largely coherent with the substrate, and the image shows no indication of a deviation from the perovskite structure, despite the large tetragonality with $c/a = 1.22$.

B. R-like-to-T-like transition of BFO and BBFO

The results for the entire series of $\text{Bi}_{0.9}\text{Ba}_{0.1}\text{FeO}_{3-\delta}$ films grown on the various substrates are shown in Fig. 2, where we again simplify the analysis by treating all films as nearly tetragonal and, therefore, plot the out-of-plane lattice parameter c as a function of the in-plane lattice

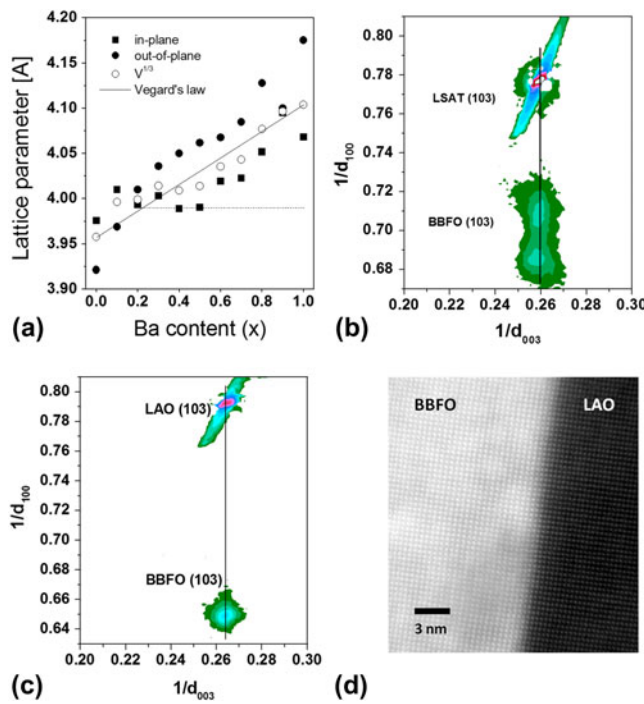


FIG. 1. (a) Lattice parameters of $\text{Bi}_{1-x}\text{Ba}_x\text{FeO}_{3-\delta}$ films. Samples for $x \geq 0.2$ were grown on SmScO_3 -buffered LaAlO_3 (LAO) substrates and for $x = 0$ and 0.1 grown directly onto KTaO_3 . The dotted horizontal line indicates the lattice parameter of the scandate buffer. Solid circles and squares correspond to out-of-plane and in-plane lattice parameters, respectively, whereas open circles indicate the corresponding pseudocubic lattice parameter ($a^2c)^{1/3}$. The linear interpolation (Vegard's law) is indicated as a guide to the eye. (b) and (c) X-ray reciprocal space maps through the film's and the substrate's 103 reflections for $\text{Bi}_{0.9}\text{Ba}_{0.1}\text{FeO}_{3-\delta}$ on $(\text{La}_{0.29}\text{Sr}_{0.71})(\text{Al}_{0.65}\text{Ta}_{0.35})\text{O}_3$ and LAO, respectively. (d) Z-contrast scanning transmission electron microscopy cross-section image of the interface between $\text{Bi}_{0.9}\text{Ba}_{0.1}\text{FeO}_{3-\delta}$ on LAO.

parameter a . Labels by the data points indicate the type of substrate on which the film was grown. This representation allows us to attribute the two different diffraction peaks within the RSMs of the films on NGO and LSAT as belonging to two different crystalline forms of the same material. In accordance to the vocabulary introduced previously⁵ for BFO, we label the less-tetragonal phase as R-like (i.e., a monoclinic structure with strong resemblance to the rhombohedral phase of BFO, even if our data are insufficient to resolve the details of the monoclinic phase beyond the comparably small c/a ratio). Similarly, we label the more highly tetragonal structure T-like. In fact, for the sample grown on LaAlO_3 , refining the structure based on the positions of 12 XRD peaks (including the accessible $00l$, $0kk$, and hhh peaks as well as 112 , 211 , and 321), the structure can be described as tetragonal with $a = b = 3.79(2) \text{ \AA}$ and $c = 4.64(3) \text{ \AA}$.

Guides to the eye are drawn as lines corresponding to a constant unit cell volume (which would overestimate the c enhancement as a consequence of strain for a realistic, compressible solid). Comparing the lines for the T-like and R-like phases indicates that compressive strain results in an abrupt increase in the unit cell volume by 4.9%.

The lower panel in Fig. 2 shows the same type of data for BFO, with a comparison of our data (solid squares) to results found in the literature. Solid lines again correspond to a constant unit cell volume, and results from LDA + U calculations⁵ are also indicated. The increase in unit cell volume ($\Delta V/V = 6.5\%$) corresponds to the previously observed monoclinic-to-monoclinic phase transition.^{5,6,12} Although the end members (on LAO and KTO substrates, respectively) behave similarly for both BFO and $\text{Bi}_{0.9}\text{Ba}_{0.1}\text{FeO}_{3-\delta}$, there is a clear difference in how this strain-induced transition occurs as the substrate's lattice parameter is reduced. For BFO, a film on an LSAT

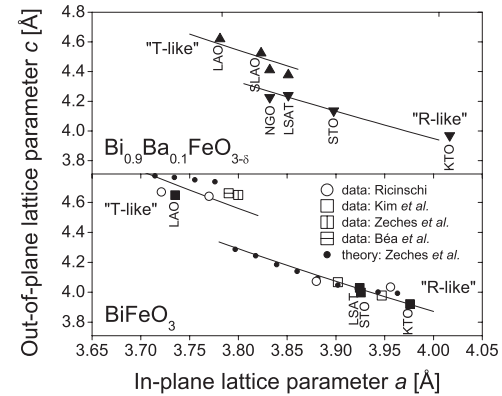


FIG. 2. Composition-dependent transition between the monoclinic "T-like" and "R-like" phases, evidenced in plots of the lattice parameters $c(a)$ for $\text{Bi}_{0.9}\text{Ba}_{0.1}\text{FeO}_{3-\delta}$ (top panel) and BiFeO_3 (BFO) (bottom). Results of this work are shown as solid symbols. The lines (drawn as guide to the eye) correspond to constant unit cell volumes ($c \propto a^{-1/2}$). For BFO, the data are compared to predictions from LDA + U calculations⁵ and previously published experimental results.^{3-5,7}

substrate grows with an in-plane lattice parameter that is significantly larger than that of the substrate (3.92 Å versus 3.86 Å) and shows a small tetragonality ($c/a = 1.03$). $\text{Bi}_{0.9}\text{Ba}_{0.1}\text{FeO}_{3-\delta}$, in contrast, almost perfectly strains to LSAT [Fig. 1(b)] and already shows the presence of the phase with the high tetragonality ($c/a = 1.13$ for this sample). In other words, the strain-induced structural transition in $\text{Bi}_{0.9}\text{Ba}_{0.1}\text{FeO}_{3-\delta}$ occurs already on substrates with a much larger lattice parameter than those needed to induce the T-like phase in BFO. Thus, the critical compressive strain σ_c necessary to induce the monoclinic-to-monoclinic phase transition is reduced significantly by the substitution of Ba for Bi. This is presumed to be a consequence of the enlargement of the unit cell volume by Ba substitution, as discussed earlier [Fig. 1(a)].

C. Temperature-dependent x-ray studies

Epitaxial strain in thin films can result from lattice mismatch at the growth temperature or from differences in thermal expansion between a substrate and a film. For example, large tensile strain is obtained on BFO films when they are grown on Si substrates.⁸ Thus, it is not a priori clear whether BFO and $\text{Bi}_{0.9}\text{Ba}_{0.1}\text{FeO}_{3-\delta}$ crystallize in the T-like phase during deposition or if these materials undergo a structural phase transition during cooling after growth. Therefore, x-ray θ -2θ scans through the film's and the substrate's 001_{pc} peaks were recorded every 50° between 100 and 750 °C for both BFO (Fig. 3) and $\text{Bi}_{0.9}\text{Ba}_{0.1}\text{FeO}_{3-\delta}$ (data not shown). The 001 reflections for the BFO and the LaAlO_3 substrate are clearly seen; the vertical “stripe pattern” between the two peaks is a consequence of thickness fringes from the film peak. The R-like phase of BFO would appear as a peak near 22.2° and is clearly not observed. At 750°, the film decomposed in air. This data thus clearly demonstrate that the T-like phase is stable up to the decomposition temperature of BFO, with the same results also observed for $\text{Bi}_{0.9}\text{Ba}_{0.1}\text{FeO}_{3-\delta}$. Interestingly, the peak position for the film shifts in the opposite direction than that of the LAO substrate with temperature, i.e., the c -axis lattice parameter for this film decreases with increasing temperature. Assuming that the in-plane registry between the film and the substrate does not change with temperature (insignificant formation of structural defects during the x-ray experiment), the film's in-plane lattice parameter is obtained by scaling the room-temperature value of a with the temperature dependence of the LAO substrate's diffraction peak (for which $a_{pc} = c_{pc}$). Thus, the unit cell volume of BFO is found to increase from 67.14 to 67.85 Å³, corresponding to a small thermal expansion of $\alpha_{\text{BFO}} = 0.58 \times 10^{-5}/\text{K}$ (while the same data set shows a thermal expansion of $\alpha_{\text{LAO}} = 1.1 \times 10^{-5}/\text{K}$ for LaAlO_3 , in agreement with published data²⁴). The low thermal expansion of BFO

(in the T-like phase) thus contributes to the tetragonal strain, but this contribution is not sufficient for the R-like-to-T-like transition. In fact, a hypothetical cubic, incompressible material with the same thermal expansion as this film and deposited at 620 °C onto LaAlO_3 would exhibit a room-temperature tetragonality of $c/a = [(1 + 600\alpha_{\text{LAO}})/(1 + 600\alpha_{\text{BFO}})]^3 = 1.01$. This again shows that the T-like structure of the film is not simply the Poisson-type consequence of an in-plane compression, consistent with the increase of unit cell volume upon compressive strain.

D. Magnetic properties of $\text{Bi}_{1-x}\text{Ba}_x\text{FeO}_{3-\delta}$

The formation of “T-like” phase films on conducting bottom electrodes has not been possible without the occurrence of significant leakage across the films, and thus it was not possible to further investigate the ferroelectric properties of these materials. R-like phase $\text{Bi}_{1-x}\text{Ba}_x\text{FeO}_{3-\delta}$ showed insulating behavior (too insulating for $R(T)$ measurements using conventional apparatus), and quantitative $P(E)$ measurements have not yet been completed.

We now turn our attention to the magnetic properties of both the T-like and R-like forms of BFO and $\text{Bi}_{0.9}\text{Ba}_{0.1}\text{FeO}_{3-\delta}$. Low-temperature data are shown in Fig. 4, where the film's magnetization is measured with the magnetic film in the plane and plotted after subtraction of the substrate's contribution as measured on a separate sample. Because of variations between different crystals, the absolute value of the magnetization is difficult to obtain on such nonsaturated loops. However, clear qualitative observations can be made. First, we note that none of the loops are fully saturated even at 6 T, indicative of magnetic ordering that can only be induced at very high fields. This is quite different from most epitaxial films of ferromagnetic perovskites, which often saturate at fields below 1 T and may be indicative of more complex order in all the samples. The differences between the T-like and R-like phases are clearly noticeable for BFO, where the

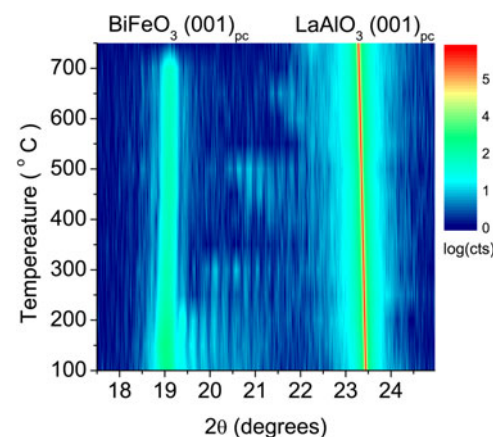


FIG. 3. Temperature dependence of the 0–20 x-ray scan through the film and substrate 001 reflections for BFO on LaAlO_3 .

induced (high-field) magnetization increases at least twofold by epitaxial strain. This hints to a different spin orientation between the two antiferromagnetic materials and is subject to further study. More strikingly, the addition of 10% Ba clearly transforms the material into a ferromagnet. In fact, the data point to a superposition of a nonsaturated (high-field) response with a more conventional ferromagnetism having a remanent magnetization of $\sim 0.1 \mu_B/\text{Fe}$ ion and a coercive field of $\sim 0.5 \text{ T}$. Without the knowledge of the exact oxygen stoichiometry δ of these $\text{Bi}_{1-x}\text{Ba}_x\text{FeO}_{3-\delta}$ films, a definite analysis of this behavior is not possible because charge neutrality in the Ba-substituted films could in principle be maintained either entirely by the formation of oxygen vacancies (for $\delta = x/2$) or by a mixed Fe valence state ($\text{Fe}^{3+}_{1-x}\text{Fe}^{4+}_x$ or $\text{Fe}^{3+}_{1-x/2}\text{Fe}^{5+}_{x/2}$).

To determine the Fe valence from XPS data, the accepted curve fitting scheme²⁵ was used to describe the Fe 2p_{2/3} line (data not shown). Although there are subtle differences between the samples, all show a predominant Fe^{3+} character, as expected for low Ba content. However, the spectra indicate a weak but clear trend to higher Fe valence with Ba substitution (implying that $\delta < x/2$). Therefore, Fe occurs in a mixed-valent state, similar, for example, to $\text{La}_{1-x}\text{Sr}_x\text{FeO}_3$ (where charge disproportionation into Fe^{3+} and Fe^{5+} is observed,^{26,27} with a predicted ferromagnetic superexchange between $\text{Fe}^{3+}:3d^5$ and $\text{Fe}^{5+}:3d^3$,²⁸) or $\text{BaFeO}_{3-\gamma}$, (where the ferromagnetic $\text{Fe}^{4+}-\text{O}-\text{Fe}^{4+}$ superexchange competes with O-vacancy-induced antiferromagnetic $\text{Fe}^{3+}-\text{O}-\text{Fe}^{4+}$ coupling.) However, at the present low value of x , the observed small average magnetic moment of $\sim 0.1 \mu_B/\text{Fe}$ may be indicative of ferromagnetic clusters within an antiferromagnetic matrix.

IV. SUMMARY AND CONCLUSIONS

To summarize, our data show that the solid solution $\text{Bi}_{1-x}\text{Ba}_x\text{FeO}_{3-\delta}$ is stable for all values $0 \leq x \leq 1$. For the specific example of $\text{Bi}_{0.9}\text{Ba}_{0.1}\text{FeO}_{3-\delta}$, we show that the critical strain σ_c needed to induce the monoclinic-to-monoclinic phase transition (from a nearly rhombohedral R-like to a nearly tetragonal T-like phase) is significantly reduced with respect to pure BFO, with the R-like and T-like phases coexisting on NGO and LSAT substrates. On LAO, both BFO and $\text{Bi}_{0.9}\text{Ba}_{0.1}\text{FeO}_{3-\delta}$ crystallize directly in the T-like phase rather than undergoing a phase transition upon cooling, i.e., the T-like phase is stable up to the temperature at which the films decompose in air ($\sim 750 \text{ }^\circ\text{C}$). Measurements of the magnetic properties show that the strain-induced structural change is accompanied by a significant increase in the induced magnetization, whereas the addition of 10% Ba results in a ferromagnetic response ($M_R \approx 0.1 \mu_B/\text{Fe}$ and $H_c \approx 0.5 \text{ T}$) superimposed to the unsaturated $M(H)$ loop as seen in BFO. These results show

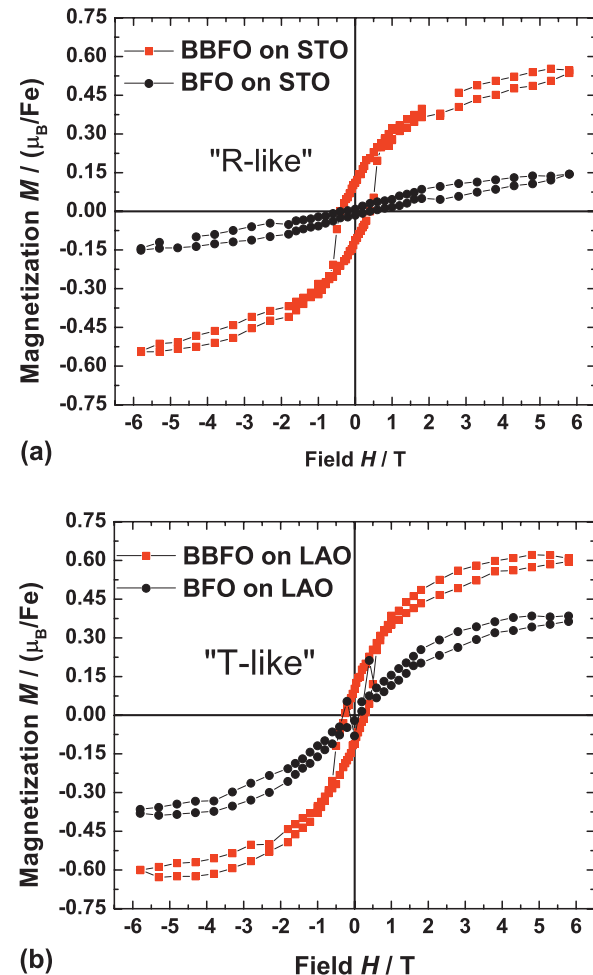


FIG. 4. Low-temperature magnetization data (taken at 5–10 K with the field in the plane) for $\text{Bi}_{0.9}\text{Ba}_{0.1}\text{FeO}_{3-\delta}$ and BFO. (a) Data in the “R-like” phase (i.e., on SrTiO_3), (b) the equivalent for the “T-like” phase (i.e., on LaAlO_3).

that small compositional changes can be used to significantly modify bismuth ferrite’s response to epitaxial strain and tune its magnetic properties.

ACKNOWLEDGMENTS

This research was supported by the U.S. Department of Energy, Basic Energy Sciences, Materials Sciences and Engineering Division (C.J.C.B., H.S.K., M.V., H.M.M., and H.M.C.), and Scientific User Facilities Division (M.D.B.). D.P.N. acknowledges support by Army Research Office and National Science Foundation under Grant No. 0704240 (AFH). We thank J.T. Luck for specimen preparation.

REFERENCES

1. J. Wang, J.B. Neaton, H. Zheng, V. Nagarajan, S.B. Ogale, B. Liu, D. Viehland, V. Vaithyanathan, D.G. Schlom, U.V. Waghmare, N.A. Spaldin, K.M. Rabe, M. Wuttig, and R. Ramesh: Epitaxial

BiFeO_3 multiferroic thin film heterostructures. *Science* **299**, 1719 (2003).

2. N.A. Hill: Why are there so few magnetic ferroelectrics? *J. Phys. Chem. B* **104**, 6694 (2000).
3. D. Ricinschi, K.-Y. Yun, and M. Okuyama: A mechanism for the $150 \mu\text{C cm}^{-2}$ polarization of BiFeO_3 films based on first-principles calculations and new structural data. *J. Phys. Condens. Matter* **18**, L97 (2006).
4. H. Béa, B. Dupé, S. Fusil, R. Mattana, E. Jacquet, B. Warot-Fonrose, F. Wilhelm, A. Rogalev, S. Petit, V. Cros, A. Anane, F. Petroff, K. Bouzehouane, G. Geneste, B. Dkhil, I. Ponomareva, L. Bellaïche, M. Bibes, and A. Barthélémy: Evidence for room-temperature multiferroicity in a compound with a giant axial ratio. *Phys. Rev. Lett.* **102**, 217603 (2009).
5. R.J. Zeches, M.D. Rossell, J.X. Zhang, A.J. Hatt, Q. He, C.-H. Yang, A. Kumar, C.H. Wang, A. Melville, C. Adamo, G. Sheng, Y.-H. Chu, J.F. Ihlefeld, R. Enri, C. Ederer, V. Gopalan, L.Q. Chen, D.G. Schlom, N.A. Spaldin, L.W. Martin, and R. Ramesh: A strain-driven morphotropic phase boundary in BiFeO_3 . *Science* **326**, 977 (2009).
6. A.J. Hatt, N.A. Spaldin, and C. Ederer: Strain-induced isosymmetric phase transition in BiFeO_3 . *Phys. Rev. B* **81**, 054109 (2010).
7. D.H. Kim, H.N. Lee, M.D. Biegalski, and H.M. Christen: Effect of epitaxial strain on ferroelectric polarization in multiferroic BiFeO_3 films. *Appl. Phys. Lett.* **92**, 012911 (2008).
8. H.W. Jang, S.H. Baek, D. Ortiz, C.M. Folkman, R.R. Das, Y.H. Chu, P. Schafer, J.X. Zhang, S. Choudhury, V. Vaithyanathan, Y.B. Chen, D.A. Felker, M.D. Biegalski, M.S. Rzchowski, X.Q. Pan, D.G. Schlom, L.Q. Chen, R. Ramesh, and C.B. Eom: Strain-induced polarization rotation in epitaxial (001) BiFeO_3 thin films. *Phys. Rev. Lett.* **101**, 107602 (2008).
9. G. Xu, H. Hiraka, G. Shirane, J. Li, J. Wang, and D. Viehland: Low symmetry phase in (001) BiFeO_3 epitaxial constrained thin films. *Appl. Phys. Lett.* **86**, 182905 (2005).
10. M.D. Biegalski, K. Dör, D.H. Kim, and H.M. Christen: Applying uniform reversible strain to epitaxial oxide films. *Appl. Phys. Lett.* **96**, 151905 (2010).
11. H. Liu, P. Yang, K. Yao, and J. Wang: Twinning rotation and ferroelectric behavior of epitaxial BiFeO_3 (001) thin film. *Appl. Phys. Lett.* **96**, 012901 (2010).
12. H.M. Christen, J.H. Nam, H.S. Kim, A.J. Hatt, and N.A. Spaldin: *Phys. Rev. B* (in press).
13. H.J. Van Hook: Oxygen stoichiometry in the compound BaFeO_{3-x} . *J. Phys. Chem.* **68**, 3786 (1964).
14. V.A. Khomchenko, D.A. Kiselev, E.K. Selezneva, J.M. Vieira, A.M.L. Lopes, Y.G. Pogorelov, J.P. Araujo, and A.L. Khoklin: Weak ferromagnetism in diamagnetically-doped $\text{Bi}_{1-x}\text{A}_x\text{FeO}_3$ ($\text{A} = \text{Ca}, \text{Sr}, \text{Pb}, \text{Ba}$) multiferroics. *Mater. Lett.* **62**, 1927 (2008).
15. V.A. Khomchenko, M. Kopcewicz, A.M.L. Lopes, Y.G. Pogorelov, J.P. Araujo, J.M. Vieira, and A.L. Khoklin: Intrinsic nature of the magnetization enhancement in heterovalently doped $\text{Bi}_{1-x}\text{A}_x\text{FeO}_3$ ($\text{A} = \text{Ca}, \text{Sr}, \text{Pb}, \text{Ba}$) multiferroics. *J. Phys. D: Appl. Phys.* **41**, 102003 (2008).
16. T. Matsui, S. Daido, N. Fujimura, T. Yoshimura, H. Tsuda, and K. Morii: Effect of Bi substitution on the magnetic and dielectric properties of epitaxially grown $\text{BaFe}_{0.3}\text{Zr}_{0.7}\text{O}_{3-\delta}$ thin films on SrTiO_3 substrates. *J. Phys. Chem. Solids* **68**, 1515 (2007).
17. V.A. Khomchenko, D.A. Kiselev, J.M. Vieira, L. Jian, A.L. Khoklin, A.M.L. Lopes, Y.G. Pogorelov, J.P. Araujo, and M. Maglione: Effect of diamagnetic Ca, Sr, Pb, and Ba substitution on the crystal structure and multiferroic properties of the BiFeO_3 perovskite. *J. Appl. Phys.* **103**, 024105 (2008).
18. H.-J. Feng and F.-M. Liu: Electronic structures and magnetoelectric properties of tetragonal BaFeO_3 : An ab initio density-functional theory study. *Chin. Phys. B* **17**, 1874 (2008).
19. E. Lucchini, S. Meriani, and D. Minichelli: An x-ray study of two phases of BaFeO_{3-x} . *Acta Crystallogr. B (Struct. Cryst. and Cryst. Chem.)* **B29**, 1217 (1973).
20. K. Mori, T. Kamiyama, H. Kobayashi, K. Oikawa, and S. Ikeda: Structural evidence for the charge disproportionation of Fe^{4+} in $\text{BaFeO}_{3-\delta}$. *J. Phys. Soc. Jpn.* **72**, 2024 (2003).
21. E. Taketani, T. Matsui, N. Fujimura, and K. Morii: Effect of oxygen deficiencies on magnetic properties of epitaxial grown BaFeO_3 thin films on (100) SrTiO_3 substrates. *IEEE Trans. Magn.* **40**, 2736 (2004).
22. C. Callender, R. Das, A.F. Hebard, J.D. Budai, and D.P. Norton: Ferromagnetism in pseudocubic BaFeO_3 epitaxial films. *Appl. Phys. Lett.* **92**, 012514 (2008).
23. H.M. Christen and G. Eres: Recent advances in pulsed laser deposition of complex oxides. *J. Phys. Condens. Matter* **20**, 264005 (2008).
24. B.C. Chakoumakos, D.G. Schlom, M. Urbanik, and J. Luine: Thermal expansion of LaAlO_3 and $(\text{La},\text{Sr})(\text{Al},\text{Ta})\text{O}_3$, substrate materials for superconducting thin-film device applications. *J. Appl. Phys.* **83**, 1979 (1998).
25. A.P. Grosvenor, B.A. Kobe, M.C. Biesinger, and N.S. McIntyre: Investigation of multiplet splitting of Fe 2p XPS spectra and bonding in iron compounds. *Surf. Interface Anal.* **36**, 1564 (2004).
26. M. Takano and Y. Takeda: Electronic state of Fe^{4+} ions in perovskite-type oxides. *Bull. Inst. Chem. Res. Kyoto Univ.* **61**, 406 (1983).
27. J.Q. Li, Y. Masui, S.K. Park, and Y. Tokura: Charge ordered states in $\text{La}_{1-x}\text{Sr}_x\text{FeO}_3$. *Phys. Rev. Lett.* **79**, 297 (1997).
28. J.B. Goodenough: *Magnetism and the Chemical Bond* (Interscience-Wiley, New York, 1963).